# MASTER

## MATHEMATICAL FINANCE

# MASTER´S FINAL WORK

## DISSERTATION

## THE rBERGOMI ROUGH VOLATILITY MODEL

## IÑIGO RESCO SAN JOSÉ

## OCTOBER - 2022

# MASTER
MATHEMATICAL FINANCE

# MASTER´S FINAL WORK
DISSERTATION

## THE rBERGOMI ROUGH VOLATILITY MODEL

IÑIGO RESCO SAN JOSÉ

**SUPERVISION:**

JOÃO MIGUEL ESPIGUINHA GUERRA

OCTOBER - 2022

ABSTRACT

Simulation schemes to estimate volatility from high frequency data lead some authors to start studying local volatility models, where the local volatility of the stock varies with the stock price and the stock price is itself stochastic. Hence, in local volatility models, volatility is stochastic, but only because it is a function of the stochastic stock price. This typically produces a skew in implied volatility (known as volatility smile), which can also be obtained by using stochastic volatility models (like, for example, the Heston stochastic volatility model), where the constant volatility of the Black-Scholes model is replaced by a stochastic process driven by a random factor correlated with the random factor that drives the price of the underlying asset.

Recently, Bayer et al. in [1] have gone a step further from local and stochastic volatility modelling, proposing rough fractional stochastic volatility (RFSV) models stating that log-volatility behaves as a fractional Brownian motion with Hurst exponent $H$ less than 0.5, which is essentially a non-Markovian process with stationary but not independent increments. As a particular case for the RFSV model, these authors proposed the so-called rough Bergomi (rBergomi) model. In this dissertation, the rBergomi model is implemented by using the hybrid scheme proposed by Bennedsen et al. in [3], and the implied volatility smiles over the SPX options are estimated for different maturities. Finally, as the model depends only on three parameters: H, $\eta$ (related to increments of log-volatility) and $\rho$ (correlation factor), these were calibrated to market data.


KEYWORDS: rough Bergomi model, fractional Brownian motion, option pricing, volatility smile

# TABLE OF CONTENTS

# ACKNOWLEDGMENTS

First of all, I would like to thank my supervisor Professor João Guerra for his continued support and guidance that enabled me to complete this research successfully.

Lastly, I want to thank my family for their unconditional support throughout these couple of years: *Ama, Aita, eskerrik asko danagatik.*

# 1. INTRODUCTION

Pricing financial derivatives, such as options, can be a thorough empirical task to mirror the trends of the option prices with the minimal error, but simulating schemes to estimate volatility of the options seeking for the market observed skew, known as volatility smile [5], is far more arduous. One of the first attempts to uniquely estimate the option prices was the Gaussian model first introduced by Fischer Black and Myron Scholes, and later developed by Robert Merton, widely known as the Black-Scholes model. The tractability of the model and the closed-form formula for the option price produced its popularity among market and academic users. However, in the Black-Scholes model the volatility is a given parameter and is assumed to be constant over time. This is not suitable to account for the estimation of observed implied volatility over different maturities and strikes (we would not achieve any volatility skew), therefore this aspect led us to consider more sophisticated approaches.

One of the first standard approaches, firstly introduced in [6] and then subsequently developed in [8] and [5], for modelling implied volatilities from high frequency data lead authors to start studying local volatility models where the local volatility of the stock varies with the stock price, and the stock price is stochastic by itself. Hence, in local volatility models, volatility is stochastic, but just because it is a function of the stochastic stock price, which it is fully correlated. In the real markets, implied and realized volatility tend to be somehow correlated with either stock price or an index, but the correlation is not complete.

Other authors went one step further following the essence within stochastic volatility models, and proposed models where the volatility parameter is replaced by a stochastic process which in turn is correlated with the stochastic process that drives the underlying asset. Within these approaches we can encounter models such as the Extended Black-Scholes (Hull White model) or the Heston model (see [12] and [11] respectively), where the volatility of the stock is set to be independently stochastic and mean-reverted.

Up until this point, one could think the studied field to be this type of stochastic volatility models as their advantages are evident in the numerous research in terms of tractability (efficiency in computation) and implied volatility surface modelling, but regarding accuracy of the simulated volatility smile over long and short maturities, one can go a step further seeking for a more accurate approach.

In general, the majority of stochastic volatility models can fit reasonably well the observed implied volatility for long expirations but the fit for short expirations is something that can be improved. The fractional Brownian motion (fBm) described in [15] was taken as a departure point. It is a centred Gaussian process whose increments, driven by the Hurst parameter $H \in (0,1)$ , are stationary but not independent except in the standard Brownian case (when H=1/2) and it is a process that is neither a semimartingale nor a Markov process. Therefore, the process in a future time $t$ does not depend only on present observation $t_0$. After taking that in consideration, the Rough Fractional Stochastic Volatility model (RFSV) was proposed in [1] and [9].

The approach of the RSFV model leads naturally to the Rough Bergomi (rBergomi) model. In the rBergomi model, the log-volatility behaves as a fBm, so the volatility process becomes non-Markovian with stationary but not independent increments. Moreover, the change of measure from $\mathbb{P}$ to the equivalent martingale measure $\mathbb{Q}$ is assumed to be deterministic. In [9], the authors showed that the RFSV model generates data remarkably consistent with empirical financial time series data. Moreover, in [1], the authors show how to use the rBergomi model to price contingent claims on the underlying asset and integrated variance. They also show that the rBergomi model fits the SPX index volatility better than Markovian stochastic volatility models using fewer parameters.

The goals of this dissertation are to discuss the main aspects of stochastic volatility and rough volatility modelling, in particular in the case of the rBergomi model. In addition, by using the hybrid scheme as in [3], the rBergomi model is computationally implemented using Python and we calibrate the model to real market data in order to evaluate if the model reproduces well the volatility smiles observed in the market.

This dissertation is organized as follows. In Chapter 2 will introduce preliminary theory concepts such as stochastic volatility models, the concept of the volatility smile and rough volatility models, considering some of their properties. In particular, we will discuss the rBergomi model. In Chapter 3, we present the main equations and describe the numerical methods applied in the simulation of the rBergomi model, after considering a change of measure from $\mathbb{P}$ to $\mathbb{Q}$. Moreover, we present some results of the simulations and compare these results with real market volatility smiles. In Chapter 4, we present a calibration procedure, we calibrate the main parameters to real market data and we compare the volatility smiles generated by the model with the real data volatility smiles. In Chapter 5 we summarize the main conclusions extracted from the whole dissertation.

## 2. PRELIMINARY THEORY

### *2.1 Background*

In our financial market model, the randomness is modelled by a probability space $(\Omega, \mathcal{F}, \mathbb{P})$ equipped with a filtration $\mathbb{F} = \{\mathcal{F}_t, t \geq 0\}$. The underlying stock price process $S = \{S_t, t \geq 0\}$ is assumed to be an adapted and continuous stochastic process defined on $(\Omega, \mathcal{F}, \mathbb{P}, \mathbb{F})$.

Before the stock market crash on the 19th of October of 1987 (known as Black Monday), the Black-Scholes model was widely used in financial institutions for pricing and hedging options. In this market model, based upon the Geometric Brownian Motion (GBM), we have the dynamics of the underlying stock price ($S_t$) characterized by the following stochastic differential equation (SDE)

$$dS_t = \mu S_t dt + \sigma S_t dW_t, \tag{1}$$

where $W = \{W_t, t \geq 0\}$ is a Wiener process or standard Brownian motion, $\mu$ is the drift and $\sigma$ the volatility of the stock returns. In this model, both $\mu$ and $\sigma$ are assumed to be constant and therefore the only source of uncertainty is $W$. By Itô stochastic calculus, we know the solution to the SDE above is

$$S_t = S_0 \exp\left( \sigma W_t + \left(\mu - \tfrac{1}{2}\sigma^2\right) t \right). \tag{2}$$

This solution, $S_t$, has lognormal distribution for every $t > 0$.

Assuming a plain vanilla option with price given by $C = C(S,t)$, as a function of stock price and time, if we apply Itô's lemma on $C$, we have that

$$dC = \frac{\partial C}{\partial t} dt + \frac{\partial C}{\partial S}(S,t) dS + \frac{1}{2}\frac{\partial^2 C}{\partial S^2}(S,t)\, dS^2. \tag{3}$$

We can consider a self-financing portfolio based on the underlying asset and the option, such that this portfolio has zero risk. In order to exclude arbitrage opportunities, the rate of return of this portfolio must be equal to the risk-free interest rate $r$. Considering this portfolio and the previous equation, we obtain that (see [2] for details)

$$\frac{\partial C}{\partial t}(S,t) + \frac{1}{2}\sigma^2 S^2 \frac{\partial^2 C}{\partial S^2}(S,t) = r\left(C - S\frac{\partial C}{\partial S}\right). \tag{4}$$

In essence, by rearranging the terms, we have the famous Black-Scholes pricing equation

$$\frac{\partial C}{\partial t} + rS\frac{\partial C}{\partial S} + \frac{1}{2}\sigma^2 S^2 \frac{\partial^2 C}{\partial S^2} - rC = 0. \tag{5}$$

Recalling that a Call Option on a particular stock with a maturity $T$ and strike price $K$ has a payoff of

$$C(S,T) = (S_T - K)^+ \tag{6}$$

and therefore, we can use this condition as the boundary condition.

After the stock crash happened, traders generally became more and more downside-risk averse as the general belief was that the probability of large downward movements was higher than having upward movements. This, among other reasons, lead to a skewness in short and long maturity options, where the implied volatility for low strike options (in the money calls and out the money puts) is higher than the implied volatility for high strike options (out the money calls and in the money puts). Therefore, it was observed that market participants have been willing to pay more for downside protection relative to equidistant out of the money upside exposure. Although this does not lead to a perfect smile with the ∪ shape, when implied volatilities and strikes are compared, the concept of "volatility smile" is widely used between practitioners to refer to this volatility skewness.

All these events could not be reconciled with the Black-Scholes constant volatility assumptions, independently of the strike and time to expiration of any option on that stock. As a consequence, local volatility models began to be studied.

### 2.2  Local volatility models

As a starting point, the local volatility market model was proposed by Bruno Dupire [6]. This one-factor type of model for the stock price $(S_t, t > 0)$ is defined as:

$$\frac{dS_t}{S_t} = rdt + \sigma(t, S_t)dW_t, \qquad\qquad S_0 > 0 \quad , \qquad (7)$$

where W is a standard Brownian motion, $r$ is the risk-free interest rate, taken as a constant in this particular case and the dividend rate $q = 0$. The diffusion coefficient $\sigma$ depends on stock price and time in this case. The issue of not capturing the skewness (the volatility smile) in the Black-Scholes pricing model trigger Bruno Dupire to extend its reasoning by stating that given a surface of European call prices $C = C(K, T)$ with maturity T and strike price K, it exists the following function $\sigma(t, S)$ such that is capable to match out those prices exactly:

$$\sigma(t, S)^2 = 2 \left. \frac{\frac{dC}{dT} + rK\frac{dC}{dK}}{K^2\frac{d^2C}{dK^2}} \right|_{\substack{K=S \\ T=t}} . \tag{8}$$

*Equation (8)* expresses the local volatility as a function of derivatives of call option prices and contains a one-dimensional Markov representation in terms of $(t, S_t)$. Historically, the local volatility model has been presented as a variant of the Black-Scholes model such that the instantaneous volatility is a deterministic function of $(t, S)$. Therefore, the pricing equation is identical to the Black-Scholes case, only with the $\sigma(t, S_t)$ distinction

$$\frac{\partial C}{\partial t} + rS\frac{\partial C}{\partial S} + \frac{1}{2}\sigma(t, S)^2 S^2 \frac{\partial^2 C}{\partial S^2} - rC = 0 \tag{9}$$

This equation is the Black-Scholes partial differential equation with the constant volatility $\sigma$ replaced by the function $\sigma(t, S_t)$. The equation can be solved by traditional numerical methods such as Monte Carlo simulation or finite difference methods, among others. By following this procedure, the calibration would be completed and therefore the local volatility model provides arbitrage-free option values.

As it was explained, the advantages of the model are its similarities to the original Black-Scholes model and its dynamics. Those resemblances with the Black-Scholes model go to an extent that, as it was shown in [5], the Black-Scholes implied volatility for a standard option can be viewed as the approximate average of the local volatility between the current stock price and the option's strike at expiration.

Although, local volatility models are not perfect, and as a matter of fact they have some disadvantages. For example, initially the local volatility function is calibrated at $t = 0$ over the market skew and kept frozen from $t$ onwards. As time goes by and the stock prices fluctuate, the market trading practitioners need to systematically recalibrate the

local volatility function on a regular basis in order to price the options with the minimal error.

In a nutshell, the local volatility model only uses prices at time $t$ and makes no assumptions about their behaviour across a time frame. The model is actually is able to fit the smile at today prices, but the model returns an almost constant smile for long maturities, leading to a flat forward smile. Therefore, it leads to unreasonable skew dynamics and underestimates the volatility of volatility. This goes far from reality, especially for exotic options which depend on the forward smile such as cliquet options and other forward starting options [10].

In contrast, to overcome the issue of behaviour of the local volatility models in a consistent and time-invariant way, the stochastic volatility models are time-homogeneous. Future skews and future volatilities of volatilities (generated by the model) are determined by the model's parameters set up at inception.


## 2.3 Stochastic volatility models

Fundamentally, a stochastic volatility model differs from the local volatility model in the sources of randomness. In local volatility, the only source of randomness was the stock price whereas in stochastic volatility models, apart from the stock price, the volatility is stochastic by itself (by definition).

Probably the most famous stochastic volatility model is the Heston model [11], where it is assumed that the dynamics of stock price is given by

$$dS_t = \mu S_t dt \ + \ \sqrt{v_t} S_t dW_t^S, \tag{10}$$

and the dynamics of the instantaneous variance is

$$dv_t = \kappa(\theta - v_t)dt \ + \ \xi\sqrt{v_t}dW_t^v, \tag{11}$$

being $W^S$ and $W^v$ Wiener processes correlated by $\rho$, $v_0$ is the initial volatility, $\theta$ is the long variance, $\kappa$ is the rate at which $v_t$ reverts to $\theta$ and $\xi$ the volatility of volatility.

The Heston model is quite tractable in computations but the volatility smile fit, crucial topic of research and main target of this dissertation, can be improved. For long expirations, it is known that the Heston model performs really well in the volatility smile

modelling [8], but for short maturities, slightly more sophisticated approaches can be followed for the optimal fit.

## 2.4 rBergomi model

One of the models that improves the approaches considered in the previous sections is the rBergomi model, derived from the RFSV model. This model starts by considering a fractional Brownian motion (fBm) (see [15]).

The fBm is a generalisation of the more well-known process of Brownian motion. It is a centred Gaussian process with stationary increments. However, the increments of the fractional Brownian motion are not independent, except in the standard Brownian case. The structure dependence of the increments is modelled by the Hurst parameter $H \in [0,1]$ and is defined as follows.

A centered Gaussian process $W^H = \{W_t^H, t \geq 0\}$ is called a fractional Brownian motion (fBm) with Hurst parameter $H \in [0,1]$ if it has the covariance function

$$R_H(t,s) = E[W_t^H W_s^H] = \frac{1}{2}(s^{2H} + t^{2H} - |t-s|^{2H}) \quad s,t \geq 0. \tag{12}$$

For a Gaussian process, its distribution is uniquely determined by its mean and covariance function. Therefore, the distribution of a fBm is uniquely specified by the above definition.

As explained in [15], *Equation (12)* is a homogeneous function of order $2H$. From this property, it can be deduced that fBm is $H$ self-similar, which means that, for $\alpha > 0$, $\{W_{\alpha t}^H, t \geq 0\}$ has the same distribution as $\{\alpha^H W_t^H, t \geq 0\}$. From *Equation (12)*, we can deduce that

$$E[|W_t^H - W_s^H|^2] = |t-s|^{2H}, \quad s,t \geq 0, \tag{13}$$

which implies that fBm has stationary increments.

The rBergomi model starts by setting the increments of the log-volatility (realized variance) in a time interval of size $\Delta$ as

$$log\ \sigma_{t+\Delta} - log\ \sigma_t = \nu\ (W_{t+\Delta}^H - W_t^H), \tag{14}$$

being $\nu$ a positive constant. Here, $\sigma = \{\sigma_t, t \geq 0\}$ denotes the volatility process, $log\ \sigma_t$ differences are the observations of the log-volatility process on a time grid with $\Delta \in [0,T]$

and $W^H$ is the fBm with Hurst parameter $H$. In [9], the authors show that for time scales of interest in finance (ranging from one day to some years), the realized variance time series are consistent with the *Equation (14)*. In particular, they show that *Equation (14)* holds for all 21 equity indices in the Oxford-Man database.

Additionally, rough volatility models are consistent with the so called "term structure at the money volatility skew": $\psi(\tau) = \left|\frac{\partial}{\partial m}\sigma_{BS}(m, \tau)\right|_{m=0}$. Here, $m = log\frac{K}{S_0}$ is the log-moneyness and $\tau$ is the time to expiry. Empirical data shows that $\psi(\tau) = \tau^{-\alpha}$, for some $\alpha > 0$ and the rBergomi model is consistent with this (see [1]). In contrast, conventional stochastic volatility models are not. On top of that, some microstructural studies of the market also showed that typical behavior of market participants at the high-frequency scale generate rough volatility [7].

Hence, we consider the Mandelbrot-Van Ness representation of fBm $W^H$ in terms of Wiener integrals, which is given by:

$$W_t^H = C_H \left\{ \int_{-\infty}^t \frac{dW_s^{\mathbb{P}}}{(t-s)^\gamma} - \int_{-\infty}^0 \frac{dW_s^{\mathbb{P}}}{(-s)^\gamma} \right\}, \tag{15}$$

where $\gamma = 1/2 - H$ and the parameter $C_H$ has the form of

$$C_H = \sqrt{\frac{2\,H\,\Gamma\,(3/2 - H)}{\Gamma\,(H + 1/2)\Gamma\,(2 - 2H)}}, \tag{16}$$

which ensures that *Equation (12)* is satisfied. Then, taking into consideration that $v_t = \sigma_t^2$ and substituting *Equation (15)* in *Equation (14)* under the measure $\mathbb{P}$, we have that

$$log\,v_u - log\,v_t$$

$$= 2\,v\,C_H \left\{ \int_{-\infty}^t \frac{dW_s^{\mathbb{P}}}{(u-s)^\gamma} - \int_{-\infty}^0 \frac{dW_s^{\mathbb{P}}}{(t-s)^\gamma} \right\}$$

$$= 2\,v\,C_H \left\{ \int_t^u \frac{1}{(u-s)^\gamma}\,dW_s^{\mathbb{P}} \right.$$

$$\left. + \int_{-\infty}^t \left[ \frac{1}{(u-s)^\gamma} - \frac{1}{(t-s)^\gamma} \right] dW_s^{\mathbb{P}} \right\}$$

$$=: 2\,v\,C_H \left\{ M_t\,(u) + Z_t\,(u) \right\}. \tag{17}$$

Note that $Z_t(u)$ is $\mathcal{F}_t$-measurable, whereas $M_t(u)$ is independent of $\mathcal{F}_t$, and Gaussian with mean zero and variance $(u - t)^{2H}/2H$. We introduce the process

$$\widetilde{W}_t^{\mathbb{P}}(u) := \sqrt{2H} \int_t^u \frac{dW_s^{\mathbb{P}}}{(u - s)^\gamma}, \tag{18}$$

which has the same properties as $M_t(u)$, with the nuance of having the variance $(u - t)^{2H}$. With $\eta := 2 v \, C_H / 2H$ we have that $2 v \, C_H \, M_t(u) = \eta \widetilde{W}_t^{\mathbb{P}}(u)$ and therefore

$$\mathbb{E}^{\mathbb{P}}[v_u | \mathcal{F}_t] = v_t \, exp \left\{ 2 v \, C_H \, Z_t(u) + \frac{1}{2} \eta^2 \mathbb{E} \big| \widetilde{W}_t^{\mathbb{P}}(u) \big|^2 \right\}. \tag{19}$$

Consequently, using the Wick stochastic exponential for a zero mean Gaussian random variable $\lambda$, defined by

$$\mathcal{E}_W(\lambda) := exp \left( \lambda - \frac{1}{2} \mathbb{E}[|\lambda|^2] \right), \tag{20}$$

we have that

$$v_u = v_t \exp \left\{ \eta \widetilde{W}_t^{\mathbb{P}}(u) + 2 v \, C_H \, Z_t(u) \right\}$$

$$= \mathbb{E}^{\mathbb{P}}[v_u | \mathcal{F}_t] \, \mathcal{E} \left( \eta \, \widetilde{W}_t^{\mathbb{P}}(u) \right). \tag{21}$$

After these considerations, we need to take into account a few aspects: the non-Markovian nature of $v_u$ is hidden in *Equation (21)* in the dependence of $Z_t(u)$ on the full history of $W^{\mathbb{P}}$ and the conditional distribution of $v_u$ depends of $\mathcal{F}_t$ only through the instantaneous variance estimates $\mathbb{E}^{\mathbb{P}}[v_u | \mathcal{F}_t], u > t$.

If the log-volatility of *Equation (14)* is modelled as a fractional Ornstein - Uhlenbeck process, we obtain a more general model: the so-called rough fractional stochastic volatility model (RFSV) model, which has the following dynamics:

$$dX_t = v \, dW_t^H - \alpha \, (X_t - m) \, dt, \tag{22}$$

$$\sigma_t = exp(X_t), \quad t \in [0, T], \tag{23}$$

which means that the model depends only on 5 parameters: $H, \alpha, m, X_0$ and $v$. Note that in the rBergomi model, we consider the particular case of $\alpha = 0$.

Finally, as a particular case for the RFSV model, the authors in [1] propose the dynamics of the underlying stock price $S_u$ and the instantaneous variance $v_u$ under the physical probability measure as

$$\frac{dS_u}{S_u} = \mu_u du + \sqrt{v_u}\, dZ_u^{\mathbb{P}}, \tag{24}$$

$$v_u = v_t \exp\left\{ \eta\, \widetilde{W}_t^{\mathbb{P}}(u) + 2\, v\, C_H Z_t(u) \right\}, \tag{25}$$

$$W^{\mathbb{P}} = \rho\, Z^{\mathbb{P}} + \bar{\rho}\, \bar{Z}^{\mathbb{P}}, \quad \rho^2 + \bar{\rho}^2 = 1. \tag{26}$$

defined in terms of two standard Brownian motions $Z_u^{\mathbb{P}}$ and $W_u^{\mathbb{P}}$ being the parameters the correlation $\rho$, $C_H$ and $\eta$. The stochastic process $\mu_u$ is a suitable drift term.

However, for option pricing on the underlying SPX at fixed time $t$, this has to be based on an equivalent martingale measure EMM $\mathbb{Q}$, that is, $\mathbb{Q} \sim \mathbb{P}$ on $[t,\ T]$ such that the discounted asset price process $\tilde{S}_t$ is a martingale under $\mathbb{Q}$ (by Girsanov theorem). In order to have a simple notation, we consider that the risk-free interest rate is $r = 0$ and therefore $\tilde{S}_t = S_t$. Therefore, under the measure $\mathbb{Q}$, we have a price dynamics given by

$$\frac{dS_u}{S_u} = \sqrt{v_u}\, dZ_u^{\mathbb{Q}}, \quad t \le u \le T,$$

considering a change of measure of the type

$$dZ_u^{\mathbb{Q}} = dZ_u^{\mathbb{P}} + \frac{\mu_u}{\sqrt{v_u}} du, \quad t \le u \le T.$$

Recall that the Volterra process in *Equation (18)* was defined in terms of $W^{\mathbb{P}}$, which is a Brownian motion correlated with $Z^{\mathbb{P}}$, according to *Equation (26)*. Note also that the components of the vector of processes $(Z^{\mathbb{P}}, \bar{Z}^{\mathbb{P}})$ are independent standard Brownian motions. A general change of measure for the second component $\bar{Z}^{\mathbb{P}}$ of *Equation (26)* is of the form

$$d\bar{Z}_u^{\mathbb{Q}} = d\bar{Z}_u^{\mathbb{P}} + \gamma_u du, \tag{27}$$

where $\gamma_u$, for $t \le u \le T$, is an adapted process called, as in [1], *market price of volatility risk*. Consequently,

$$dW_u^{\mathbb{Q}} = dW_u^{\mathbb{P}} + [\rho\, \mu_u / \sqrt{v_u} + \bar{\rho}\, \gamma_U] du, \quad t \le u \le T, \tag{28}$$

which can be expressed as

$$dW_s^{\mathbb{P}} = dW_s^{\mathbb{Q}} + \lambda(s) ds. \tag{29}$$

The so-called rough Bergomi (rBergomi) model is obtained if we consider that the process $\lambda(s)$ in *Equation (29)*, driving the change of measure, is a deterministic function. Summarizing, the dynamics of the rBergomi model under the equivalent martingale measure $\mathbb{Q}$ are given by (see [1] for more details):

$$\frac{dS_u}{S_u} = \sqrt{v_u}\, dZ_u^{\mathbb{Q}}, \qquad t \le u \le T, \tag{30}$$

$$Z_u^{\mathbb{Q}} = \rho W_u + \sqrt{1-\rho^2}\, W_u^{\perp},$$

$$v_u = \mathbb{E}^{\mathbb{P}}[v_u | \mathcal{F}_t]\, \mathcal{E}\left(\eta\, \widetilde{W}_t^{\mathbb{Q}}(u)\right) \tag{31}$$

$$\times\, \exp\left\{\eta\, \sqrt{2\,H} \int_t^u \frac{1}{(u-s)^\gamma}\, \lambda(s)\, ds\right\}$$

$$= \xi_t(u)\, \mathcal{E}\left(\eta\, \widetilde{W}_t^{\mathbb{Q}}(u)\right),$$

$$\xi_t(u) = \mathbb{E}^{\mathbb{P}}[v_u | \mathcal{F}_t]\, \exp\left\{\eta\, \sqrt{2\,H} \int_t^u \frac{1}{(u-s)^\gamma}\, \lambda(s)\, ds\right\}, \tag{32}$$

where $\rho$ is the correlation between volatility moves and price moves, $\lambda(s)$ is a deterministic function which specifies a deterministic change of measure and $\xi_t(u)$ is the forward variance curve. The processes $W$ and $W^{\perp}$ are independent standard Brownian motions. This rBergomi model is non-Markovian in the instantaneous variance $v_u$ but is Markovian in the (infinite-dimensional) state vector $\mathbb{E}^{\mathbb{Q}}[v_u | \mathcal{F}_t] = \xi_t(u)$.

Assuming the deterministic change of measure between $\mathbb{P}$ and $\mathbb{Q}$ specified by the deterministic function $\lambda(s)$, we have defined the rBergomi model. This model depends only on the forward variance curve $\xi_t(u)$ and the three parameters H, η and ρ. Our goal is to simulate the rBergomi model in order to price options and obtain the volatility smile.

## 3. SIMULATION AND NUMERICAL METHODS

In this Chapter, our goal is to incorporate and apply numerical methods, using the hybrid scheme proposed in [3], to the rBergomi model discussed in Chapter 2 and see if the model can produce volatility smiles that are qualitatively similar to the smiles observed in real market data.

As a departure point for our rBergomi model simulation algorithm, let $n$ be the number of time steps and $N$ the number of simulations. We define the Volterra process $W^\alpha$ and the Brownian motion $B$ (before was $Z$). In order to relate these processes with the ones defined in the previous chapter, see *Equation (18)* and *(30)-(32)*.

$$W_t^\alpha := \widetilde{W}_0^{\mathbb{Q}}(t) = \sqrt{2H} \int_0^t \frac{dW_u}{(t-u)^\gamma} = \sqrt{2\alpha+1} \int_0^t (t-u)^\alpha dW_u \tag{33}$$

$$B_u := Z_u^{\mathbb{Q}} = \rho W_u + \sqrt{1-\rho^2}\, W_u^\perp, \tag{34}$$

where $\alpha = H - 1/2$.

In order to simulate the Volterra process of *Equation (33)*, we consider the first order variant $(j = 1)$ of the hybrid scheme developed in [3], to capture the explosion of the kernel function close to zero. We start by considering a Brownian semi-stationary process of the type:

$$X(t) := \int_{-\infty}^t g(t-u)\ \sigma(u)dW_u\ , \qquad t \in \mathbb{R} \tag{35}$$

where $\sigma$ is an $\{\mathcal{F}_t\}_{t \in \mathbb{R}}$-predictable process with locally bounded trajectories and $g$ is a Borel-measurable kernel function. In order to ensure that the process in *Equation (35)* is well defined, we assume that the kernel function $g$ is square-integrable, meaning that $\int_0^\infty g(x)^2\, dx < \infty$. Apart from this assumption, further secondary technical considerations need to be taken into account, as explained in [3].

Under this scheme, we approximate $g$ using an appropriate power function near zero and a step function elsewhere. The subsequent discretization scheme can be realized as a linear combination of Wiener integrals with respect to the driving Brownian motion $W$ and a Riemann sum. This is precisely the reason why we call it a hybrid scheme. By applying the hybrid scheme to *Equation (35),* we have

$$X(t) = \sum_{k=1}^{\infty} \int_{t-k/n}^{t-k/n+1/n} g(t-u) \; \sigma(u) dW_u$$

$$\approx \sum_{k=1}^{\infty} \sigma\left(t - \frac{k}{n}\right) \int_{t-k/n}^{t-k/n+1/n} g(t-u) \; dW_u \quad . \tag{36}$$

If k is small, then consider the approximation

$$g(t-u) \approx (t-u)^\alpha \, L_g\left(\frac{k}{n}\right), \quad (t-u) \in \left[\frac{k-1}{n}, \frac{k}{n}\right] \backslash \{0\}, \tag{37}$$

where $L_g$ is a function varying less than the power function $x \mapsto x^\alpha$ close to zero. If $k$ is large, or at least $k \geq 2$, then choosing $b_k \in [k-1, k]$ provides the approximation

$$g(t-u) \approx g\left(\frac{b_k}{n}\right), \quad (t-u) \in \left[\frac{k-1}{n}, \frac{k}{n}\right]. \tag{38}$$

Hence, ultimately we have

$$X(t) \approx \sum_{k=1}^{j} L_g\left(\frac{k}{n}\right) \sigma\left(t - \frac{k}{n}\right) \int_{t-k/n}^{t-k/n+1/n} g(t-u)^\alpha dW_u$$

$$+ \sum_{k=j+1}^{\infty} g\left(\frac{b_k}{n}\right) \sigma\left(t - \frac{k}{n}\right) \int_{t-k/n}^{t-k/n+1/n} dW_u \quad . \tag{39}$$

After developing the basic steps within the hybrid scheme, as stated before, this method is used to simulate the Volterra process *(Equation 33)*. In order to proceed with the simulation of the Volterra process $W_t^\alpha$, we consider the first order variant ($j = 1$) of the hybrid scheme adapted to Equation (33). The scheme is specified by

$$W_{t_i}^\alpha \approx \sqrt{2\alpha + 1} \left( \int_{\frac{i-1}{n}}^{\frac{i}{n}} \left(\frac{i}{n} - u\right)^\alpha dW_u \right.$$

$$\left. + \sum_{k=2}^{i} \left(\frac{b_k}{n}\right)^\alpha \left( W_{\frac{i-(k-1)}{n}} - W_{\frac{i-k}{n}} \right) \right), \tag{40}$$

with

$$b_k := \left( \frac{k^{\alpha+1} - (k-1)^{\alpha+1}}{\alpha + 1} \right)^{\frac{1}{\alpha}}, \tag{41}$$

which minimizes the asymptotic mean square root, as explained in [4]. The points $t_i = \frac{i}{n}$. are the points of our time grid in the simulation: $\left\{ \frac{i}{n}, i = 0,1,2, \dots, [Tn] \right\}$. The increments of the standard Brownian motion are simulated by generating appropriate normal random variables.

From *Equation (33)* it is clear that $E[W_t^\alpha] = 0$ and $Var[W_t^\alpha] = t^{2\alpha+1}$. Some examples of sample paths, the expected value and variance graphical representations can be seen in *Figure 1* for a couple of maturities.
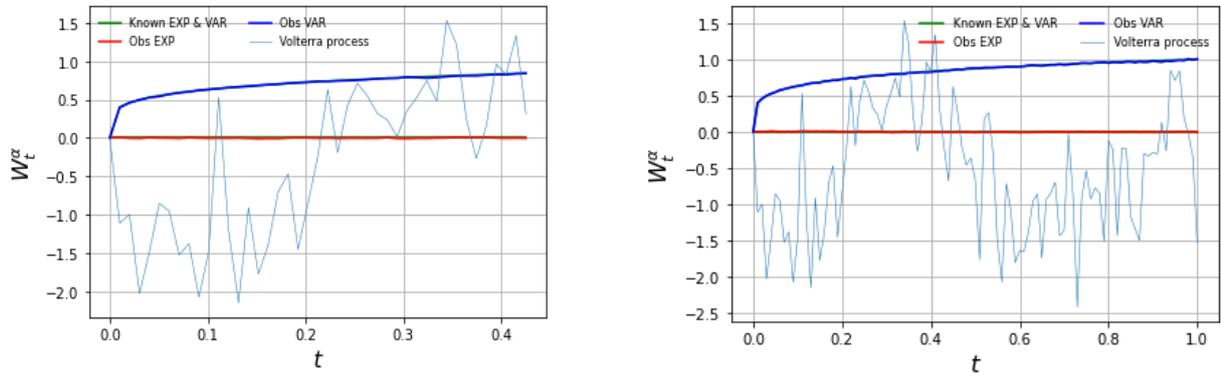


*Figure 1: Examples of sample paths of Volterra processes, its expected values and variances for maturities T=0.425 and T=1.0.*

After simulating the Volterra process $W_t^\alpha$, we use the values obtained in order to calculate the variance process. We set up the variance process $v = \{v_t, t \geq 0\}$, given by (see *Equation (31)*)

$$v_t = \xi_0(t) \, exp \left( \eta \, W_t^\alpha - \frac{\eta^2}{2} t^{2\alpha+1} \right), \tag{42}$$

which depends on the forward variance curve $\xi_0(t)$ which is considered flat, consistently with [1] ($\xi_0(t) = \xi = 0.055$). The remaining parameters $\eta > 0$ and $\rho \in [-1,1]$ can be deliberately chosen. The variance process is simulated just by using the simulated values of the Volterra process $W_t^\alpha$. In *Figure 2,* we present trajectories of variance processes, their variances and the constant expectation.
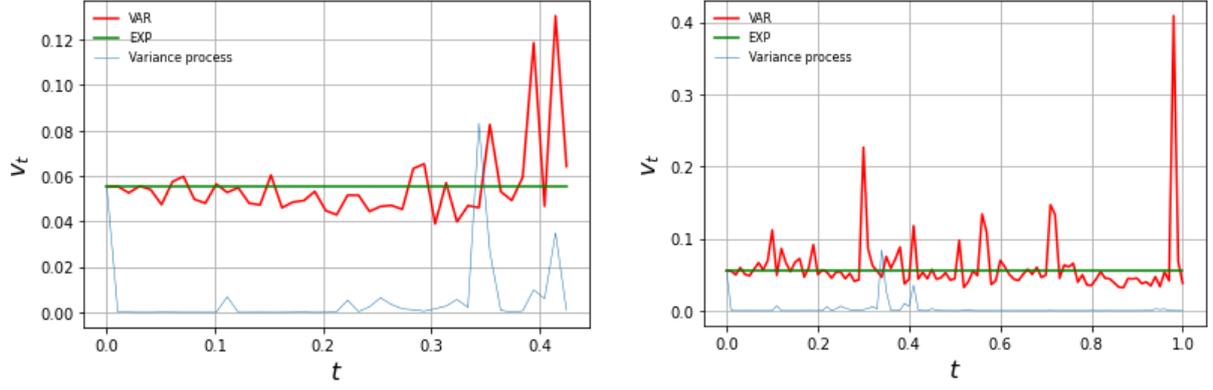
14

*Figure 2: Examples of sample paths of Variance processes, its expected values and variances for maturities T=0.425 and T=1.0.*

Then we consider the price process $S = \{S_t, t \geq 0\}$, given by (see *Equation (30)*)

$$S_t := S_0 \, exp\left\{\int_0^t \sqrt{v_u} \, dB_u - \frac{1}{2}\int_0^t v_u du\right\}, \qquad (43)$$

which depends on $S_0$, which is the initial price value. In order to simulate the price process, we consider a simple Euler scheme corresponding to the stochastic differential equation (*Equation (30)*):

$$S_{t_i} = S_{t_{i-1}} + \sqrt{v_{t_{i-1}}} \; S_{t_{i-1}} \left(\rho\big(W_{t_i} - W_{t_{i-1}}\big) + \sqrt{1 - \rho^2}\big(W_{t_i}^\perp - W_{t_{i-1}}^\perp\big)\right),$$

where the increments of the Brownian motion processes are generated by appropriate normal random variables. Note that the increments of the Brownian motion $W$ are the same that were used in the simulation of the Volterra process (see *Equation (40)*). Again, the points $t_i = \frac{i}{n}$. are the points of our time grid in the simulation: $\left\{\frac{i}{n}, i = 0,1,2, \ldots, [Tn]\right\}$.

In our examples, we will set $S_0$ to be equal to the S&P 500 price on the 25/06/2021 (4280.7 USD). From *Equation (43)* it is clear that $E[S_t] = 4280.7$ as it is shown in *Figure 3*, with a couple of simulated random price processes.
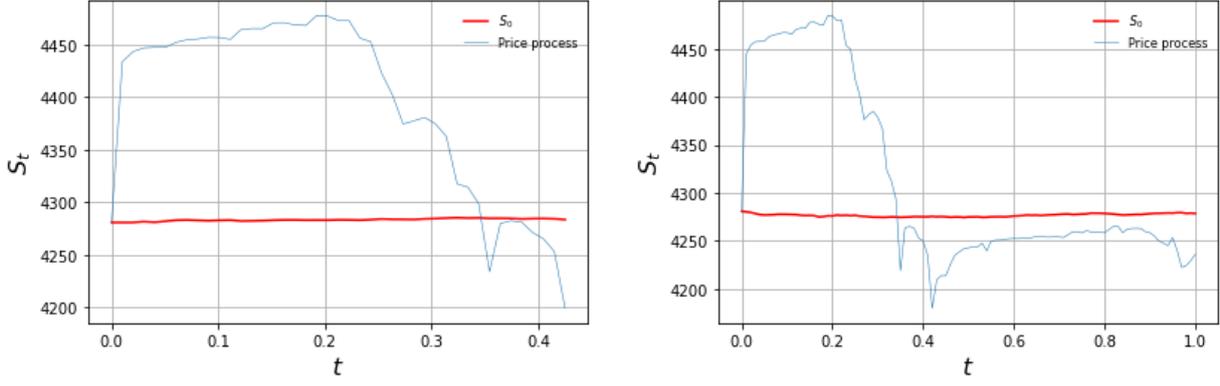
15

*Figure 3: Examples of sample paths of Price processes and its expected values for maturities T=0.425 and T=1.0.*

As a test for the price and variance processes and, following the approach in [3], we consider a log-price process representation

$$-2\mathbb{E}[log\ S_t] = \int_0^t \mathbb{E}[v_u]\,du - 2log\ S_0 = \xi t - 2log\ S_0,$$ (44)

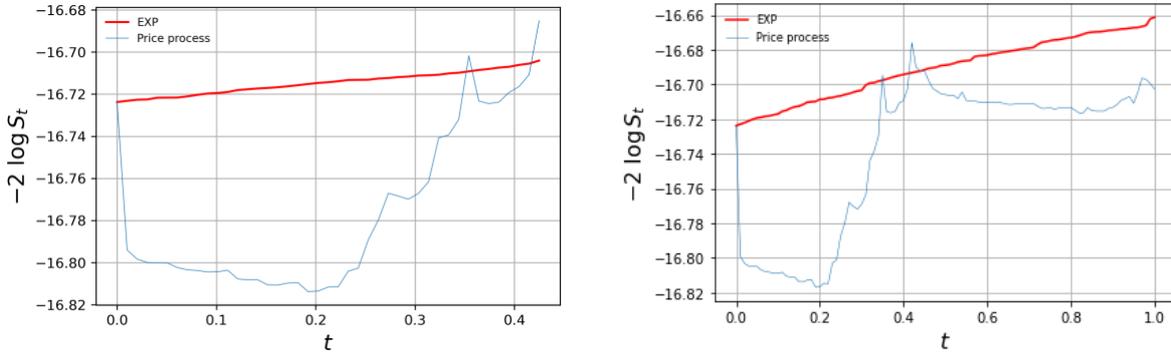which, as can be seen in *Figure 4*, enables us to cross-check the start and finish points of expected log prices, for random samples of log-prices.



*Figure 4: Examples of Log Price processes and its expected values for maturities T=0.425 and T=1.0.*

Once the price process is set, we can pass to option pricing representation. Recall that an European call/put option with maturity $T$ and log strike $k$ is defined by the payoff:

$$(S_T - e^k)^+ := \max(S_T - e^k, 0),$$ (45a)

$$(e^k - S_T)^+ := \max(e^k - S_T, 0).$$ (45b)

Let $C(S,T)$ and $P(S,T)$ be the Black-Scholes call and put option prices for non-dividend paying stock options. Assuming $r = 0$, we have the following Black-Scholes formulas:

16

$$C(S,T) := S\mathcal{N}(d_1) - e^k\mathcal{N}(d_2), \tag{46a}$$

$$P(S,T) := e^k\mathcal{N}(-d_2) - S\mathcal{N}(-d_1), \tag{46b}$$

where $\mathcal{N}(\cdot)$ represents the Gaussian cumulative distribution function and $d_2$ and $d_1$ are established as

$$d_1 := \frac{1}{\sigma\sqrt{T}}\left[ln\left(\frac{S}{e^k}\right) + T\left(\frac{\sigma^2}{2}\right)\right], \tag{47a}$$

$$d_2 := d_1 - \sigma\sqrt{T}. \tag{47b}$$

Hence, the observed rBergomi prices for call and put options are defined respectively as follows:

$$C^{Berg}(k,T) = \mathbb{E}[(S_T - e^k)^+] \approx \frac{1}{N}\sum_{i=1}^{N}(S_T^i - e^k)^+, \tag{48a}$$

$$P^{Berg}(k,T) = \mathbb{E}[(e^k - S_T)^+] \approx \frac{1}{N}\sum_{i=1}^{N}(e^k - S_T^i)^+. \tag{48b}$$

Then the implied volatilities $\sigma_{BS}(k,t)$ for the observed prices are calculated by inverting the appropriate Black-Scholes formula

$$\sigma_k^{Berg}(T) = BS^{-1}(C^{Berg}(k,T)), \tag{49a}$$

$$\sigma_k^{Berg}(T) = BS^{-1}(P^{Berg}(k,T)). \tag{49b}$$

Graphically, in *Figure 5* we can glimpse the implied volatilities (volatility smiles) for random samples of options with the calibrated parameters in Chapter 4.
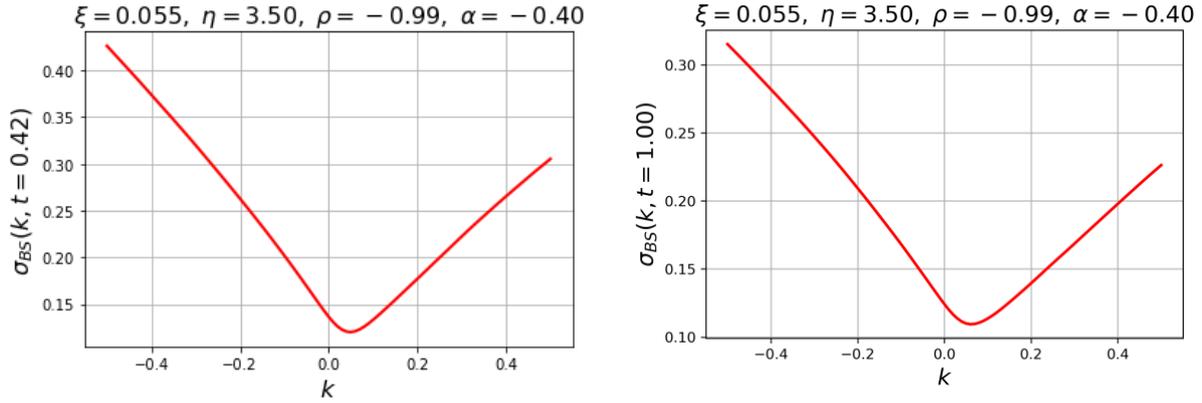
*Figure 5: Examples of Implied volatilities (volatility smiles) for maturities T=0.425 and T=1.0.*

Even though the parameters can be guessed in practice, in this case the parameters chosen for the simulation were the ones used by Bayer et al. (2016) in [1]: $\alpha = -0.43$, $\eta = 1.9$ and $\rho = -0.9$. The decision was consistently made as their behaviour in the mentioned study was quite accurate and the stock price was the same (SPX), even though the dates were different.

Summarizing, the simulation of the rBergomi model is based on the equations in this Chapter and, more particularly, depends on the three parameters set in the paragraph above. Each parameter has its own function within the model: the volatility smile depends fundamentally on $\eta$, the skewness on $\rho$ and the explosion, of both smile and skew, on $\alpha$.

In order to start running the simulation process, we have to take into account a few considerations in terms of space and time. We consider maturities $(T)$ from a week of time $(T = 0.022)$ up to a year and a half $(T = 1.564)$, for granularity we set up the 365 days of a year $(n = 365)$, 30000 paths $(N = 30000)$ and log-moneyness $k$, with its range adjusted depending on each maturity in order to capture the smile.

The real implied volatilities correspond to the SPX options of the 28/06/2021 extracted from Yahoo Finance. On that day the stock market closed at 4280.7 USD. From those real values of the options, some measures are also taken. For instance, options with implied volatilities close to zero and strike prices over a range of 50% up and down the stock price defined above, were excluded from the database and were not taken into account in the approach. After that, in order to be able to compare the real data with the estimated implied volatilities, the real strike prices were standardized by taking the logarithm of the strike prices over the initial value of the underlying asset (index value), i.e., the log-moneyness.

After those considerations, we run the code in Python (adapted from [14]) to calculate all the steps within the rBergomi model and ultimately estimate the implied volatilities for each maturity (*Tmat* in the figures) and type of option: Calls and Puts. In the following figures it is shown the real volatilities (in multicolour dots) and estimated implied volatilities (in black line), for 3 different maturities.

In *Figure 6* it is shown a sample of the rBergomi estimated implied volatilities versus the SPX real implied volatilities for call options. Overall, the model was capable to draw the volatility smile. Nevertheless, it can be seen that the model was able to capture the pronounced skewness, although in the area around the vertex the estimation could be more accurate. As maturities get larger, the volume data decreases and the shape is captured but the implied volatilities were slightly overestimated.
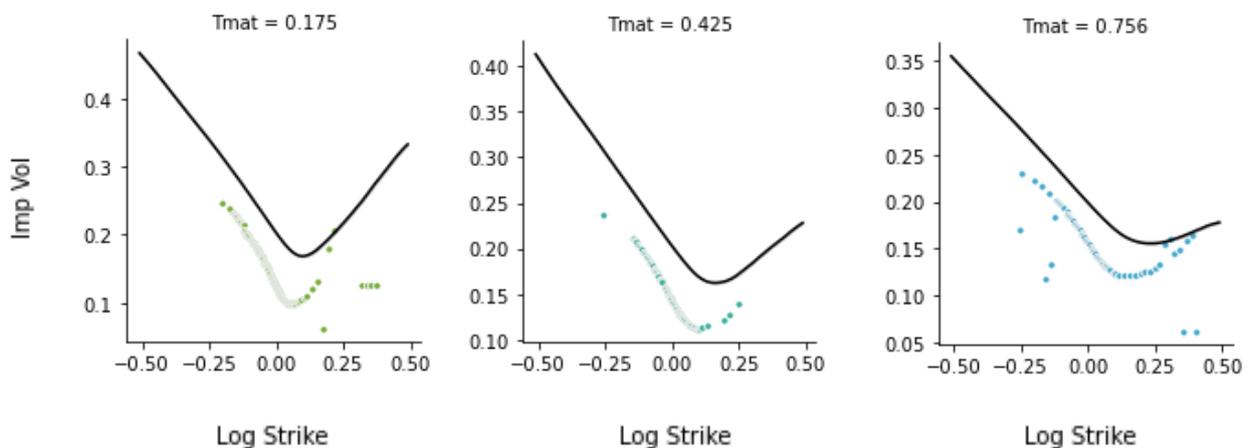


*Figure 6: Sample of SPX Calls vs rBergomi implied volatilities*

In *Figure 7* it is shown a sample of rBergomi estimated implied volatilities versus the SPX real implied volatilities for put options. Same as what happened with the calls, in general the model was capable to draw the volatility smile but in this case the approach was more accurate. Nevertheless, it can be seen for lower maturities the model was able to capture the pronounced skewness, although it was still unable to estimate with high accuracy in the area around the vertex. For longer maturities, even though the volume data decreases as maturities go by, the approach is considerably more accurate than in calls as the shape and skewness reflected very precisely the profile of the real data.
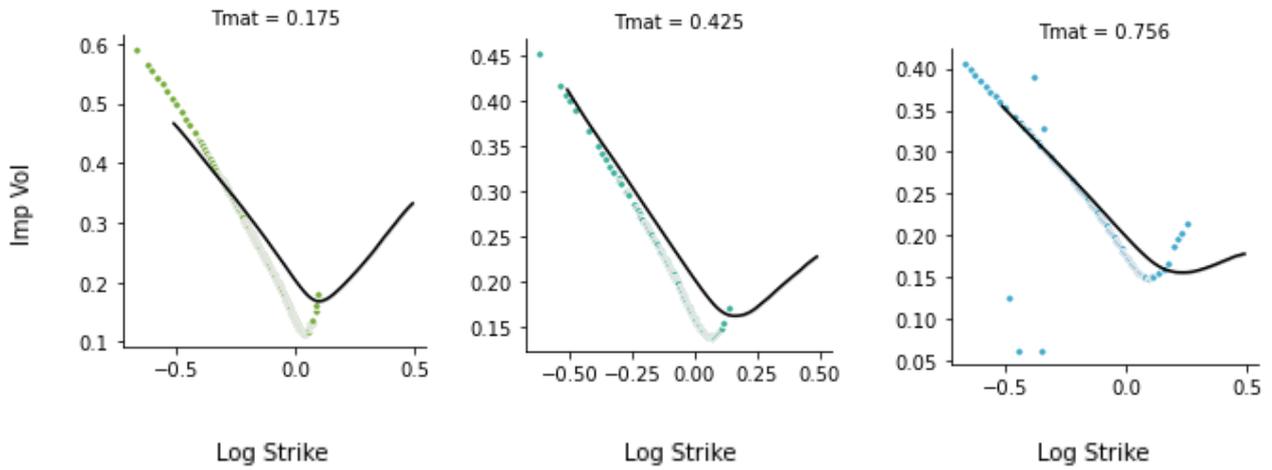
*Figure 7: Sample of SPX Puts vs rBergomi implied volatilities*

We can conclude that the qualitative features of the volatility smiles are captured by the model for all the maturities, but it is quite clear that the fit was more accurate for the puts rather than the calls.

# 4. CALIBRATION

After the simulation of the implied volatilities with the parameters and assumptions considered in Chapter 4 and after plotting them with the actual SPX Call option data, it is clear that exists a margin of improvement in the approach. The improvement on the accuracy to fit better the market data, starts by considering different values in the parameters to see if with the new values the result gets more precise.

The goal now is to minimize the differences between the rBergomi and the real implied volatilities, a standard procedure usually applied in these kind of studies. If we consider the model's dependency on just three parameters $(H, \eta, \rho)$ and the implications on the implied volatilities, when the parameters change (explained at the end of Chapter 3), we could adjust the parameters for the optimal fit.

In the calibration procedure, as it was done in [4], the following objective function was considered, and the target was to minimize the sum of the squared differences between rBergomi generated implied volatilities and real implied volatilities:

$$\sum_k \left( \sigma_k^{Berg}(H, \eta, \rho) - \sigma_k^{Real} \right)^2. \tag{50}$$

The simulation procedure started by setting up a range and a distance step in each parameter of the model (see *Diagram 1*) as well as the full set of 10 maturities with a decent amount of real data (from 0.022 up to 1.564), and across all the possible combinations between them, assuming constant the forward variance $\xi_0(t) = \xi = 0.055$. These ranges were set based on previous numerical calibrations presented in the literature (see for instance [1])

$$\begin{cases} H \in (0, 0.2] \, ; \\ \eta \in [1\,,7] \, ; \\ \rho \in [-0.999\,,-0.8] \, ; \, . \end{cases}$$

*Diagram 1: Considered ranges for the parameters in calibration*

Once the simulation is finished, the optimal parameters that were able to minimize the function in *Equation (50)* were extracted and saved for the parametrization and comparison criteria. The optimal parameters that minimized *Equation (50)* were $H = 0.1$ $\eta = 3.5$ and $\rho$ = -0.995. To see visually the optimal fit of the parameters, in *Figure 7* can be seen the SPX implied volatilities and the rBergomi generated volatilities for the range of maturities proposed before.

By comparing *Figure 8* with *Figure 6* it is clear that for those three maturities, the new parameters improved the fit into the real implied volatilities data, especially for medium maturities, possibly because the volume of the real SPX data is more concentrated in the medium maturities and, therefore the rBergomi estimation and subsequent calibration is more accurate. Nonetheless, this optimization does not only apply only for the maturities considered in *Figure 6*, it is applied for all of the maturities.
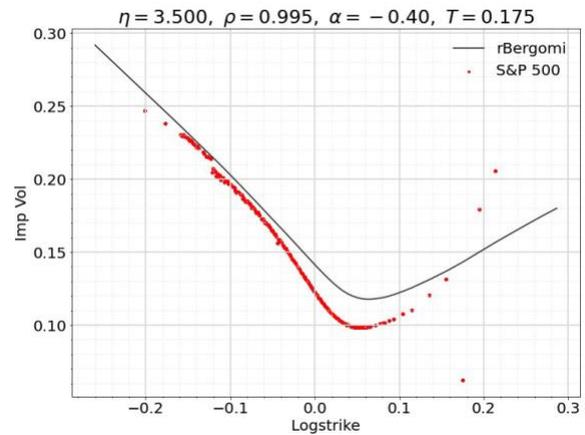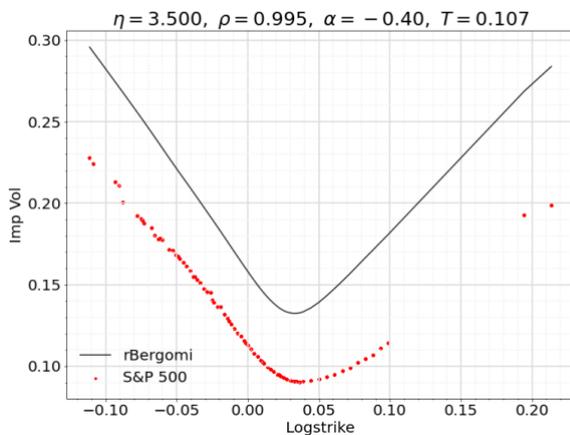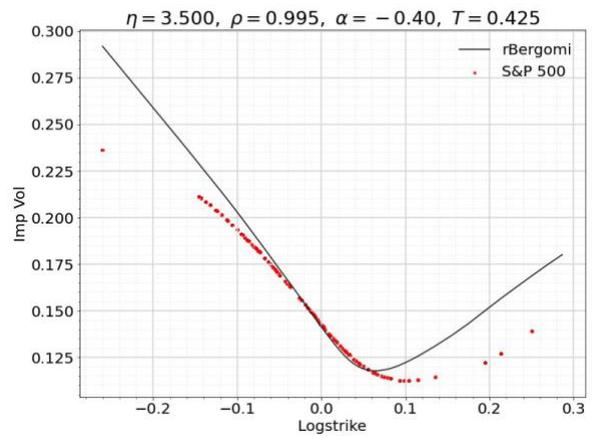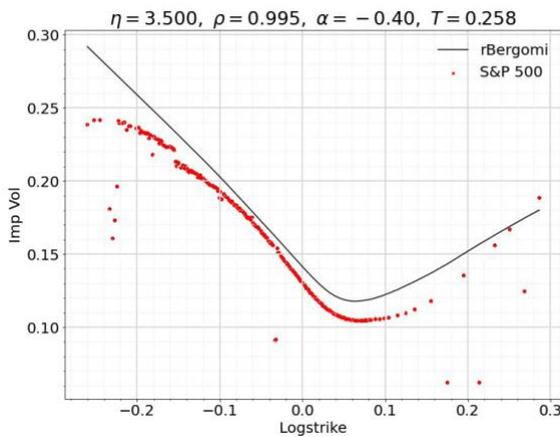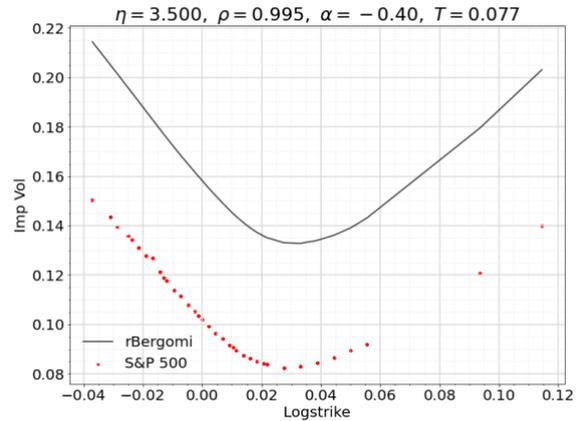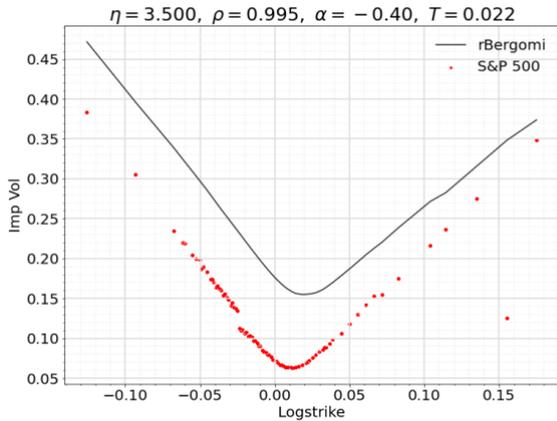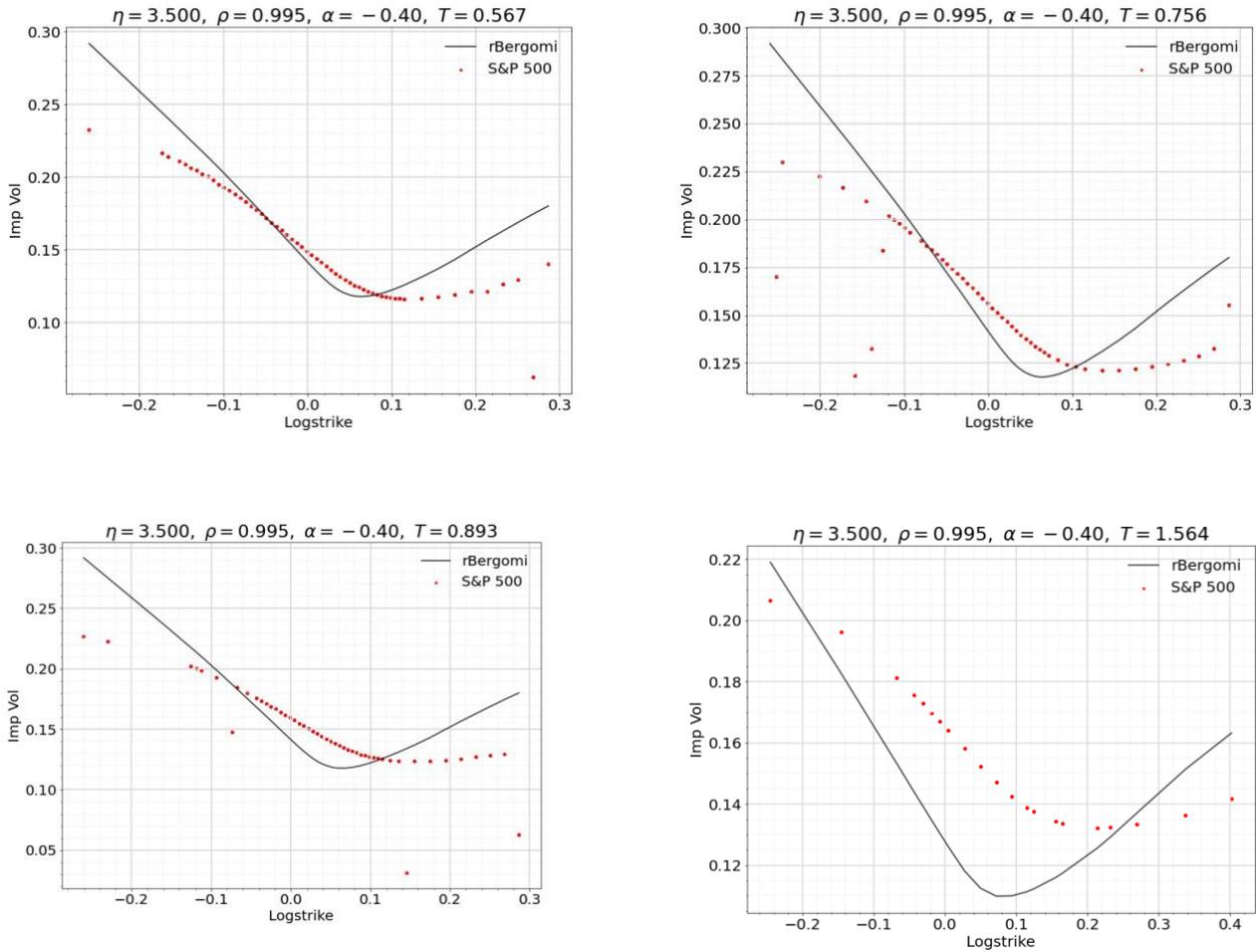
*Figure 8: Optimal calibrated rBergomi vs SPX Call volatility smiles*

A reason that might be the cause of the weak calibration results for very short and large maturities is the performance of the objective function in those maturities. Perhaps the function has different local minima and we are obtaining a local minimum and not the global one. The calibration procedure can also be substantially improved by considering sophisticated algorithms for minimizing the objective function, such as the algorithm implemented in Python by *scipy.optimize.least_squares*, which solves a nonlinear least-squares problem with bounds on the variables. These issues may justify the problem that for some maturities the quantitative values of the volatility smiles is improvable as there are significative deviations from the real data, even though qualitatively the shape is achieved. One could also consider the flat forward variance $\xi_0(t) = \xi$ as another parameter of the model to be calibrated by minimizing the objective function. This would improve substantially the quality of the fit into the market data.

With the analysis and optimization carried out in this chapter, the revised conditions should be taken into consideration for future parametrization criteria with other option data. Whenever option data changes in terms of type, index or day among others, it immediately requires a recalibration of the model for the optimal approach.

# 5. CONCLUSIONS

In this master thesis we have studied the rBergomi model fundamentals and its practical application (using the hybrid scheme developed by [3]) to real market data in order to evaluate how well the model describes the SPX implied volatility smiles. Following the previous approaches in [1] and [9] by assuming a change of measure between physical probability measure $\mathbb{P}$ to the equivalent martingale measure $\mathbb{Q}$, we confirmed that simulated data using the rBergomi model showed a decent fit into the SPX implied volatility data.

The tractability of the model, understood as the capacity of the user to modify the standard parameters; the robustness, understood as the lack of breaks in the simulations and the flexibility of the model enabled the calibration of the parameters $(H, \eta, \rho)$, in order to improve the fit in the SPX call options by minimizing the difference between the real and simulated implied volatilities. As a result, the model is capable of reproducing the shape and skewness of the real data over a range of different maturities. The volatility smiles produced by the model can reproduce the qualitative shape of the real market volatility smiles. However, for some maturities, the quantitative values of the implied volatilities were not very accurate. There is some margin for improvement in the calibration procedure by using more sophisticated least squares minimization algorithms. One could also consider the flat forward variance curve as another parameter of the model that should be calibrated by minimizing the objective function.

As we showed in this dissertation, with the rough Bergomi model, practitioners with some knowledge of simulation methods can estimate implied volatilities for a specific option, as well as stock prices, variance processes or option prices, just by applying the formulas presented in Chapter 3 in a programming tool such as Python.

The characteristics of the model and the implied volatility simulation allow the user to explore future applications of the rBergomi model, for instance, by changing the index or stock option or the option trading type.

Other more sophisticated rough volatility models can also be used in order to fit the SPX volatility smile, such as stochastic Volterra models or rBergomi models with a regime switching change of measure (stochastic change of measure). The joint calibration problem of these models to the SPX volatility smile and the VIX index volatility smile is also an important research open problem that can be studied in the future.

REFERENCES

[1] Christian Bayer, Peter Friz & Jim Gatheral. (2016). Pricing under rough volatility, Quantitative Finance, 16:6, 887-904, DOI: 10.1080/14697688.2015.1099717

[2] Thomas Bjork. (2009). Arbitrage Theory in Continuous Time, Oxford University Press, 3rd edition.

[3] Mikkel Bennedsen, Asger Lunde & Mikko S. Pakkanen. (2017). Hybrid scheme for Brownian semistationary processes , Finance Stoch 21, 931–965 (2017). https://doi.org/10.1007/s00780-017-0335-5

[4] Pierre-Alexis Corpechot. (2020). Study of the joint S&P 500/VIX smile calibration problem within rough volatility models. MSc Thesis, Imperial College London

[5] Emanuel Derman and Michael B. Miller. (2006). The Volatility Smile. John Wiley & Sons, Hoboken, Chapters 19-22

[6] Bruno Dupire. (1994). Pricing with a smile. Risk, 7(1):18-20,1994.

[7] El Euch, Fukasawa and M. Rosembaum (2018), The microstructural foundations of leverage effect and rough volatility, Finance and Stochastics, 22, 241-280

[8] Jim Gatheral. (2006). The Volatility Surface: A Practitioner's Guide. John Wiley & Sons, Hoboken, Chapters 1-3

[9] Jim Gatheral, Thibault Jaisson & Mathieu Rosenbaum (2018). Volatility is rough, Quantitative Finance, 18:6, 933-949, DOI: 10.1080/14697688.2017.1393551

[10] Eyup Gulsun. (2020). Which one is your volatility — Constant, Local or Stochastic?, Towardsdatascience. https://towardsdatascience.com/which-one-is-your-volatility-constant-local-or-stochastic-61508ef560c1

[11] Steven L Heston. (1993). A closed-form solution for options with stochastic volatility with applications to bond and currency options. Review of Financial Studies. 6 (2): 327–343. doi:10.1093/rfs/6.2.327. JSTOR 2962057

[12] J. Hull & A. White (1987). The pricing of options on assets with stochastic volatilities. Journal of Finance, 42, pp. 281-300.

[13] Antoine Jacquier. (2017). Advanced Methods in Derivatives Pricing with application to volatility modelling, Imperial College London, MSc in Mathematics and Finance Lecture notes

[14]  Ryan McCrickerd & Mikko S. Pakkanen. (2018). Turbocharging Monte Carlo pricing for the rough Bergomi model, Quantitative Finance, 18:11, 1877-1886, DOI: 10.1080/14697688.2018.1459812

[15]  Tommi Sottinen. (2003). Fractional Brownian motion in finance and queueing. Ph.D. Thesis, University of Helsinki.